Carbohydrate Polymers 99 (2014) 748–754

Contents lists available at ScienceDirect

Carbohydrate Polymers

journal homepage: www.elsevier.com/locate/carbpol

Synthesis and characterization of photochromic azobenzene cellulose ethers

Zhijun Li, Dong Zhang, Jiabao Weng, Biao Chen, Haiqing Liu*

Fujian Provincial Key Laboratory of Polymer Materials, College of Material Science and Engineering, Fujian Normal University, Fujian 350007, China

ARTICLE INFO

Article history:
Received 28 May 2013
Received in revised form 20 August 2013
Accepted 28 August 2013
Available online 5 September 2013

Keywords:
Cellulose
Azo polymers
Photochemistry
Photochromic behavior

ABSTRACT

Photochromic azobenzene cellulose ethers were prepared by homogeneous etherification of cellulose with 2,3-epoxypropoxy-azobenzene (EA) in *N*,*N*-dimethylacetamide/lithium chloride solution. The EA with epoxy group could highly efficiently react with cellulose to synthesize 3-azobenzyloxy-2-hydroxypropyl-cellulose (Azo-cellulose) ethers with controllable degree of substitution (DS_{azo}). The DS_{azo} was in a range of 0.2–2.0 adjusted by the molar ratio of EA to anhydroglucose unit of cellulose. The Azo-celluloses with $DS_{azo} \geq 0.53$ were soluble in aprotic solvents like dimethylsulfoxide. Their chemical structures and properties were characterized by elemental analysis, FT-IR, NMR, and thermogravimetric analysis. They showed reversible *trans-cis-trans* transition when Azo-cellulose/DMAc solutions were irradiated by successive irradiation of UV and visible light. The transition between *trans*- and *cis*- isomers could be effectively controlled by simply adjusting the irradiation time. The photo-stimulated *trans-cis-trans* conformational change induced conformation transition between rod-like shape of *trans*-isomer and skewed shape of *cis*-isomer.

© 2013 Elsevier Ltd. All rights reserved.

1. Introduction

Photoresponsive polymers are very interesting materials whose structure undergoes reversible change under the stimulation of non-invasive and easy available light with appropriate wavelength, leading to variation of its physical properties such as color, shape, dimension, solubility, and viscosity. Such polymers have displayed applications in many fields such as photonics, optical storage, controlled medicine delivery and release, surface relief gratings, photoswitchable biomaterials and actuators. Therefore the synthesis, characterization and application of photoresponsive polymers have attracted much research attention from both the academic and industrial circles (Ercole, Davis, & Evans, 2010; Hou, Zhang, & Wang, 2012; Li, Keller, Li, Wang, & Brunet, 2003; Nishi, Namari, & Kobatake, 2011; Pieroni, Fissi, Angelini, & Lenci, 2000).

Among the many photoresponsive polymers, azo-polymers bearing azobenzene moieties have been extensively studied (Hurduc, Adès, Belleney, Siove, & Sauvet, 2007; Xue, Zhu, Zhang, Zhang, & Zhu, 2009). The azobenzene moiety has *trans*- and *cis*-photoisomers. The former is a more stable state in visible light. Under excitation of ultraviolet light, the *trans*- changes to *cis*- structure. A reversible change occurs, i.e. *cis*- to *trans*- isomer, when irradiated with visible light or heat (Oertel, Mart, Komber, & Bohme, 2009; Sahu, Saha, & Bera, 1995). This characteristic feature makes azo-polymers useful in many new materials, such as optical memory, optical switch and information converter.

When azo-polymers are used as biomaterials such as photo-regulated in vivo drug carriers, the issues of biocompatibility and biodegradability are highly important (Ciardelli et al., 2013). Grafting of azobenzene molecules onto biopolymers provides a promising solution for the preparation of biocompatible and biodegradable photochromic materials (Asanuma et al., 2007; Hua et al., 2004). Cellulose is one of the most abundant naturally occurring biopolymers in the world. Due to the good mechanical property, biocompatibility and biodegradability, cellulose has become an important biomaterial (Chang & Zhang, 2011). Its broad applications in novel fields would inevitably lessen the depletion of fossil fuels, and relieve the environmental pollution caused by synthetic polymers. Cellulose molecular chain is composed of anhydroglucose unit (AGU) linked by β-1,4-glycosidic bond. Each AGU has three hydroxyl groups, which are reactive groups with azobenzene compounds to fabricate cellulose derivatives with chromophores. So far, a few photochromic azo-cellulose derivatives prepared by the esterification reaction have been reported (Arai & Kawabata, 1995; Arai, Shitara, & Ohyama, 1996; Yashima, Noguchi, & Okamoto, 1995). However, cellulose derivatives with photochromic moieties linked by ether bond have been less studied. An azocellulose linked by 4-cyanophenylazophenol was prepared via Mitsunobu reaction, which was a heterogeneous reaction and took a long reaction time (2 days) (Yang et al., 2001).

* Corresponding author. Tel.: +86 591 83404938; fax: +86 591 83404938.
E-mail address: haiqing.liu@gmail.com (H. Liu).

0144-8617/$ – see front matter © 2013 Elsevier Ltd. All rights reserved.
http://dx.doi.org/10.1016/j.carbpol.2013.08.093

Because of cellulose ethers are more stable than cellulose esters in basic conditions, and the preparation conditions for cellulose ethers are more ambient (like allowance of the presence of H_2O and O_2) than those for cellulose esters when esterification reagents like acryl chlorides and acid anhydride are used. In this work, cellulose was reacted with 2,3-epoxypropoxy-azobenzene through homogeneous etherification reaction in a solvent of *N*,*N*-dimethylacetamide/lithium chloride (DMAc/LiCl). The structure was studied using elemental analysis, FT-IR, ^{1}H NMR, and ^{13}C NMR spectroscopy. The photochromic property in dilute DMAc solutions, i.e. *trans-cis-trans* photoisomerization processes upon light irradiation was studied by UV–vis spectroscopy.

2. Experimental

2.1. Materials

Cellulose powder (CF11, Whatman) was used as received. Its molecular weight was ca. 3.1×10^4 g/mol measured with gel permeation chromatography (GPC) (Glasser, Becker, & Todd, 2000). *N*,*N*-Dimethylacetamide (DMAc), *N*,*N*-dimethylformamide (DMF), dimethyl sulfoxide (DMSO), 1,2-epoxy-3-chloropropane (ECP), aniline, phenol, benzyltrimethylammonium chloride (TMBAC), anhydrous lithium chloride (LiCl), sodium nitrite ($NaNO_2$), concentrated hydrochloric acid solution (36.5 wt.%), methylene chloride, chloroform and sodium hydroxide flake were purchased from Sinopharm Chemical Reagent Co., Ltd., Shanghai, China. All chemicals are of analytical grade.

Cellulose powder and LiCl were vacuum dried at 120 °C for about 12 h before use. DMAc was refluxed overnight at 80 °C in the presence of calcium hydride (CaH_2), followed by vacuum distillation. Then it was stored in a desiccator and kept over 3 Å molecular sieves. All the other reagents were used as received.

2.2. Synthesis of 2,3-epoxypropoxy-azobenzene (EA)

Following a procedure similar to that reported by Yin and coauthors (Yu, Jiang, Wang, & Yin, 2010), EA was synthesized by diazo-coupling reaction between aniline and phenol in the presence of sodium nitrite and hydrochloric acid and the following reaction with ECP in the presence of the phase transferring agent TMBAC and sodium hydroxide (Scheme 1a and b).

The yield of HA was ca. 93%. ^{1}H NMR (400 MHz, $CDCl_3$, δ ppm): 5.57 (1H, —OH), 6.93, 7.49, 7.87 (aromatic, 9H). ^{13}C NMR (400 MHz, $CDCl_3$, δ ppm): 158.48, 152.88, 147.37 130.67, 129.27, 125.20, 122.77, 116.03. FTIR spectrum (cm^{-1}, KBr pellet): 3400 (υ_{O-H}), 3157 (υ_{Ar-H}), 1600 ($\upsilon_{C=C}$), 1502 ($\upsilon_{N=N}$), and 600–850 (γ_{C-H}) for the benzene ring.

The yield of EA was ca. 60%. ^{1}H NMR (400 MHz, $CDCl_3$, δ ppm) (Fig. 1a): 2.76 and 2.90 (d, 2H, $^{c'}$H), 3.37 (m, 1H, $^{b'}$H), 4.00 and 4.28 (d, 2H, ^{a}H), 7.02 (d, 2H, ^{b}H), 7.48 (m, 3H, ^{d,e}H), 7.90 (d, 4H, ^{c}H). ^{13}C NMR (400 MHz, $CDCl_3$, ppm) (Fig. 1b): δ = 44.87 ($^{c'}$C), 50.20 ($^{b'}$C), 69.20 ($^{a'}$C), 161.06 (^{a}C), 152.34 (^{e}C), 147.53 (^{d}C), 130.63 (^{h}C), 129.26 (^{g}C), 125.20 (^{c}C), 122.82 (^{f}C), 116.03 (^{b}C). FTIR spectrum (KBr pellet) (cm^{-1}): the assignment of most peaks could be referred to that of HA, an additional typical peak at 2925 cm^{-1} was assigned to υ_{as} of —CH_2— on the epoxypropyl group.

2.3. Synthesis of 3-azobenzyloxy-2-hydroxypropyl-cellulose (Azo-cellulose)

Cellulose/DMAc-LiCl solution was prepared according to a standard procedure. Briefly, cellulose (1.5 g) was suspended in 66 g of DMAc which was pre-heated to 150 °C in N_2 atmosphere, and kept at this temperature for 30 min under stirring. Then the mixture was cooled to 110 °C, followed by an addition of 7.5 g of LiCl. After the mixture was stirred for 1 h at this temperature, it was cooled to room temperature and stirred for ca. 12 h to obtain a transparent 2 wt.% cellulose solution.

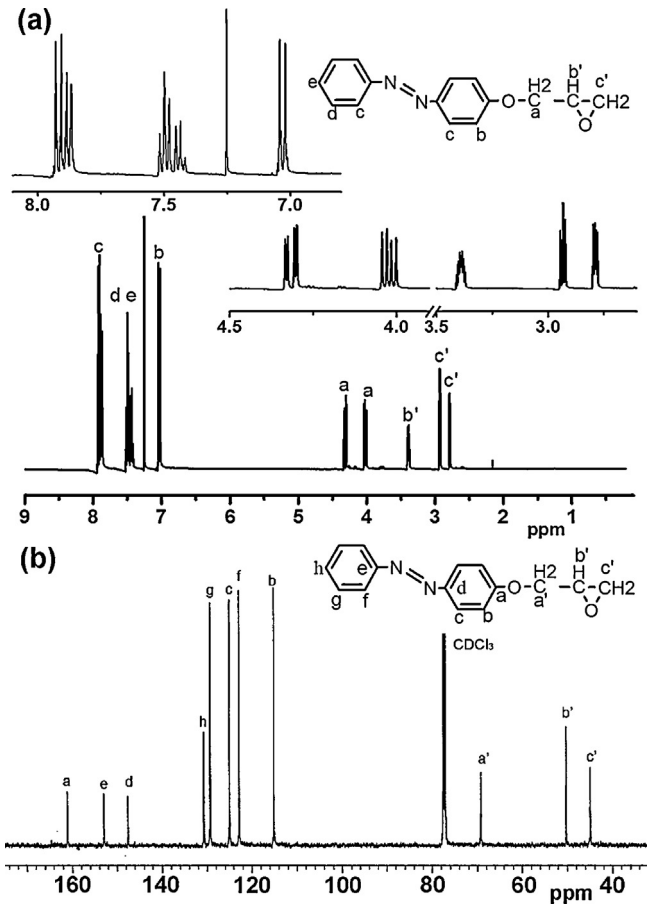

Fig. 1. (a) ^{1}H NMR and (b) ^{13}C NMR spectra of EA in $CDCl_3$.

Azo-cellulose was synthesized according to Scheme 1c. In a typical procedure to prepare Azo-cellulose1, 0.5 mL of distilled water was dropwise added to 20 g of the above prepared cellulose solution containing 0.4 g of cellulose (2.47 mmol AGU), then 1.23 g of NaOH powder (mole ratio of NaOH/AGU = 10) was added and stirred for 1 h at room temperature. Subsequently the reaction mixture was heated to 70 °C and stirred for 0.5 h. Then 0.95 mL of EA/DMAc solution with concentration of 2.6 mol/L was dropwise added and reacted for 7 h at 70 °C (mole ratio of EA/AGU = 1.0). The reaction was terminated by pouring the solution into 200 mL of diethyl ether. The precipitates were collected by filtration, and were purified by Soxhlet extraction with acetone. The products were vacuum dried at 70 °C for 12 h, and showed slight yellow color. The mass yield of Azo-cellulose1 ($m_{Azo\text{-}cellulose}/m_{cellulose} \times 100\%$) was 105%. A set of eight samples were prepared by adjusting the EA/AGU mole ratio in a range of 1–21 (Table 1). Their mass yield was in a range of 105–320%. It increased with the degree of substitution (DS) of azobenzene moiety.

2.4. Characterization

^{13}C NMR spectra of HA, EA, and Azo-cellulose samples were recorded on an AVANCE III spectrometer at 25 °C operating at 500 MHz. ^{1}H NMR spectra were carried out on a Bruker-ARX 500 spectrometer at 22 °C operating at 400 MHz. Thermal gravimetric analysis (TGA) was performed on a TA5200/MDSC291 thermogravimetric analyzer at a heating rate of 10 °C min^{-1} from 30 to 600 °C

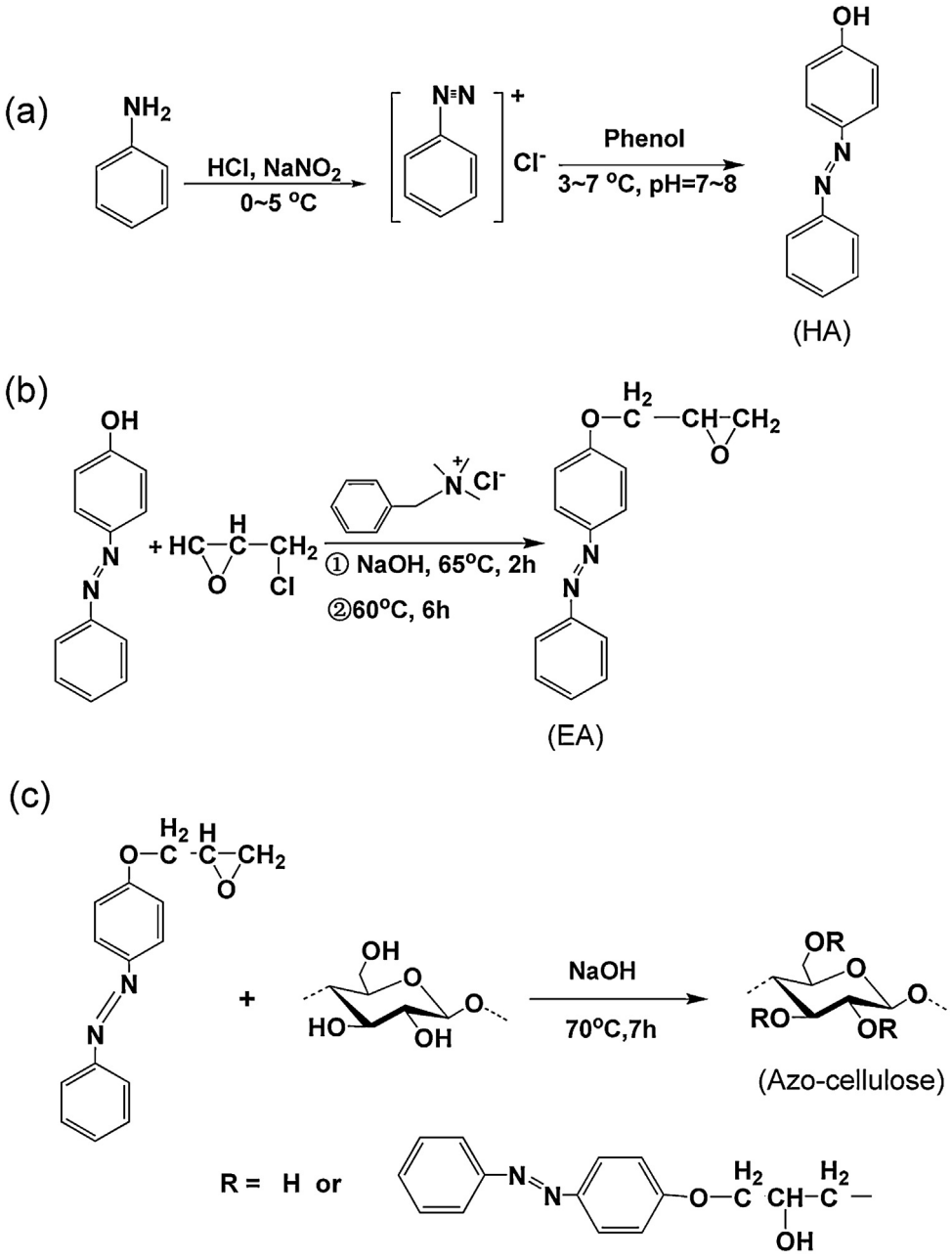

Scheme 1. Synthetic route of (a) HA, (b) EA and (c) Azo-cellulose.

Table 1
Nitrogen, carbon content, and DS_{azo} values of azobenzene cellulose (Azo-cellulose).

Sample	Mole ratio of EA/AGU	N%	C%	DS_{azo} values calculated from		
				N%	^{1}H NMR[a]	Colorimetric method[b]
Cellulose	0	0	210	0	–[c]	–[d]
Azo-cellulose1	1	2.35	48.5	0.17	–[c]	–[d]
Azo-cellulose2	3	3.33	50.0	0.28	0.26	0.20
Azo-cellulose3	6	5.01	52.0	0.53	0.58	0.48
Azo-cellulose4	9	5.33	55.4	0.60	0.63	0.53
Azo-cellulose5	12	5.88	56.4	0.73	0.68	0.61
Azo-cellulose6	15	6.36	58.6	0.87	0.83	0.75
Azo-cellulose7	18	7.01	60.0	1.11	1.03	0.86
Azo-cellulose8	21	8.34	63.8	1.98	2.03	1.88

[a] Calculated from ^{1}H NMR spectra of Azo-cellulose2–7/DMSO-d_6 and Azo-cellulose8/$CDCl_3$.
[b] Measured by the calorimetric method on basis of the absorbance at 355 nm on the UV–vis spectra, EA was used as a model compound to get the calibration curve.
[c,d] Not measured due to insolubility in DMSO and DMAc, respectively.

in nitrogen atmosphere. FTIR spectra in KBr form were performed on a Nicolet 5700 Fourier transform infrared spectrometer. Nitrogen and carbon content were measured on an elemental analyzer (Vario EL III, Hanau, Germany). The DS_{azo} was calculated according to the following equation:

$$DS_{azo} = \frac{162 \times (N\%/100)}{28 - 254.3 \times (N\%/100)}$$

where N% is the nitrogen content of Azo-cellulose. The DS_{azo} values were listed in Table 1.

The solubility of Azo-cellulose was measured by adding 0.01 g of Azo-cellulose to 10 ml of solvents like DMAc, DMF, DMSO, acetone, and chloroform, then stirred at 50 °C for 24 h. Dissolution was determined by visual inspection of the disappearance of Azo-cellulose particles. The molecular weight of Azo-celluloses was measured on Waters 1515 gel permeation chromatography with DMF as solvent and eluent, polystyrene was used as standard.

Light absorption of HA, EA and Azo-cellulose solutions in DMAc with concentration of 0.12 g/L was recorded on UV–vis spectrophotometer (Lambda 850, PerkinElmer) in a range of 250–600 nm at 28 ± 2 °C. DMAc was used as a reference. In an attempt to measure the DS_{azo} by the calorimetric method, a calibration curve ($y = 0.152x - 0.06$, $R^2 = 0.994$) was obtained by plotting the absorbance at 355 nm against concentration of model compound EA in DMAc (concentration range: 0.01–0.16 g/L). The amount of azo moieties in the Azo-cellulose was determined according to the absorbance A_{355} of the Azo-cellulose/DMAc solution. A similar method was applied for an azocellulose reported by Yang and coworkers (Yang et al., 2001). Such obtained DS_{azo} values were listed in Table 1.

Photochromic property of Azo-cellulose in solution was measured as follows. The Azo-cellulose/DMAc solution was irradiated with 365 nm light with light intensity of 20 mW/cm^2 for certain time period, then its light absorption spectrum was recorded immediately. When the spectrum reached equilibrium, the solution was irradiated under visible light of >450 nm in wavelength with light intensity of 35 mW/cm^2 for certain time interval. The light source was an incandescent lamp equipped with a long-pass filter, followed by recording of light absorption spectrum.

3. Results and discussion

3.1. Synthesis of EA

In the reaction mixture of EA synthesis, ECP acted as both a reactant and a solvent, so its content was much higher than HA, namely the mole ratio of ECP/HA was 10. HA-OH was altered to HA-O$^-$Na$^+$ after reaction with NaOH, and the HA-O$^-$ readily reacted with the epoxide group of ECP. The epoxy ring was closed with the help of NaOH and therefore EA was yielded. The phase transferring agent TMBAC was used to accelerate the reaction and improve the yield. The reaction procedure is shown in Scheme 1b. The ^{1}H NMR, ^{13}C NMR and FTIR spectra of EA are displayed in Fig. 1. Compared to the ^{1}H NMR of HA, new resonance groups at 2.76–2.90, 3.37, 4.00–4.28 ppm appear for the protons of the epoxypropyl group. The resonance at 5.57 ppm for the hydroxyl proton is completely absent, suggesting that the hydroxyl group is fully reacted with ECP to produce EA (Fig. 1a). ^{13}C NMR spectrum (Fig. 1b) shows new resonances at 44.87, 50.20, 69.20 ppm for the carbons of epoxypropyl group. The resonance for ^{a}C shifts from 158.48 to 161.06 ppm after the hydroxyl group of HA altered to epoxypropoxy group of EA, while the others appear at almost the corresponding positions to those of HA, confirming that EA is produced.

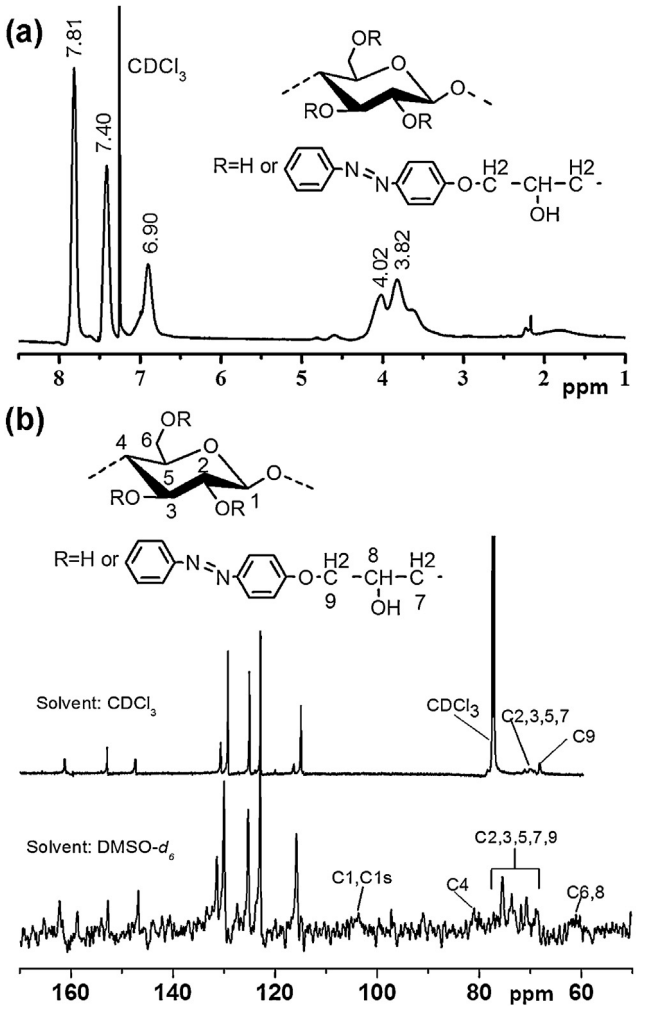

Fig. 2. (a) ^{1}H NMR and (b) ^{13}C NMR spectra of Azo-cellulose8 (DS_{azo} = 1.98) in $CDCl_3$ or DMSO-d_6.

3.2. Synthesis of Azo-cellulose

According to a procedure established by Kondo and coauthors for effectively producing cellulose ethers in solvent LiCl/DMAc (Kondo & Gray, 1991), a small amount of water was added to the cellulose/DMAc-LiCl solution, in order to allow more NaOH dissolve in the solution. By doing so, the hydroxyl group on cellulose (Cellu-OH) can be effectively activated to react with the epoxy group of EA to produce Azo-cellulose, as shown in Scheme 1c. Due to the steric hindrance effect of the azo side group, further reaction of EA with —OH group in the side chain is less likely and is not considered here. The DS_{azo} value can be controlled by adjusting the EA/AGU ratio, and a set of Azo-celluloses with DS_{azo} value in a range of 0.17–1.98 (measured by elemental analysis) were synthesized as listed in Table 1.

Fig. 2 displays ^{1}H NMR ($CDCl_3$), ^{13}C NMR (DMSO-d_6, $CDCl_3$), and FTIR spectra of Azo-cellulose8. ^{1}H NMR (Fig. 2a): the three sharp peaks at δ = 6.90, 7.40, 7.81 ppm are assigned to the protons on the aromatic azobenzene rings, the broad peak at δ = 3.2–4.8 ppm is for protons on the AGU ring, methylene and methylidyne groups (Zhang et al., 2012). Through integration area, the DS_{azo} value on the cellulose AGU was calculated by the following equation and was listed in Table 1. The three sets of DS_{azo} values calculated from nitrogen content, proton NMR and colorimetric method are close,

suggesting all the three methods are effective in obtaining the DS_{azo} values.

$$\frac{9DS_{azo}}{10+14DS_{azo}} = \frac{A_{6.90}+A_{7.40}+A_{7.81}}{A_{6.9}+A_{7.40}+A_{7.81}+A_{3.0-5.0}}$$

where A is the integrated peak area.

^{13}C NMR spectra (Fig. 2b) were obtained from two solvents, i.e. $CDCl_3$ and DMSO-d_6. Compared to the ^{13}C NMR spectrum of EA (Fig. 1b), the resonances in the range of 110–170 ppm are assigned to the carbons on azobenzene rings. Both spectra from the DMSO-d_6 and $CDCl_3$ solvents display almost identical peak signals in the 110–170 ppm range. However, the characteristic peaks in the range of 60–105 ppm for the carbons in the AGU of cellulose molecules are apparent in the spectrum from solvent DMSO-d_6 (Fox, Li, Xu, & Edgar, 2011; Zhang et al., 2012), while only weak and broad peak signals in the range of 60–80 ppm were present for C2,3,5,7 in the AGU of cellulose molecules, and C9 in the azobenzene moiety in the spectrum from solvent $CDCl_3$. This is probably due to the very strong peak at δ = 77.4 ppm of $CDCl_3$ overlaps and shields the resonances arising from the carbons in the AGU. Compared to cellulose, FTIR spectrum (not shown here) of Azo-cellulose8 shows several stronger and new absorption peaks at 2920 cm^{-1} (υ_{as} of $-CH_2-$ of epoxypropyl), 3060 cm^{-1} (υ_{Ar-H}) and 1600 cm^{-1} ($\upsilon_{C=C}$) for benzene ring, and 1500 cm^{-1} ($\upsilon_{N=N}$). These results prove that azobenzene moieties are successfully introduced onto cellulose through etherification reaction. The Mw of the Azo-cellulose (4–8) which are soluble in DMF was measured by GPC (Waters 1515). It was in a range of 2.7–2.8 $\times 10^4$ g/mol, showing that there was slight reduction in molecular weight as compared to 3.1 $\times 10^4$ g/mol of cellulose. The heat and NaOH may cause some thermal degradation and hydrolysis in the 7 h course of etherification reaction.

3.3. Solubility of Azo-cellulose

Cellulose itself hardly dissolves in conventional solvents due to strong intra- and inter-molecular hydrogen bonds (Song, Sun, Zhang, Zhou, & Zhang, 2008). After derivatization with azobenzene side chains, its solubility obviously changes with DS_{azo} value. All Azo-celluloses could not dissolve in acetone without dependence on DS_{azo} value. Azo-cellulose1–3 with DS_{azo} of 0.17–0.53 even cannot dissolve in highly polar solvent like DMAc and DMF, whereas Azo-cellulose4–8 with DS_{azo} value of 0.6–1.98 are soluble in those aprotic solvents. Azo-cellulose8 is soluble in a less polar solvent chloroform. Apparently their solubility highly depends on the DS_{azo} value. For Azo-cellulose with low DS_{azo} value, the inter- and intra-hydrogen bonding interactions of Azo-cellulose molecular chains are still very strong, resulting in insolubility of Azo-cellulose1–3 in solvent DMAc etc. Such hydrogen bonding interactions decrease with increasing DS_{azo} value, because of the steric hindrance caused by the large azobenzene side groups, leading to improved solubility, as compared to the insolubility of cellulose in any common solvents. Good solubility can benefit the processing of Azo-cellulose in solution.

3.4. Thermal stability of Azo-cellulose

Fig. 3 shows the TG thermograms of Azo-celluloses and cellulose. Before sharp weight loss, all samples including EA, cellulose and Azo-celluloses underwent 4–6% weight loss, which was dedicated to the evaporation of water absorbed on them. The pyrolysis of EA started at 195 °C, where its azo bond (N=N) was decomposed into volatile N_2, benzene and aniline (Barton et al., 1983). An additional slight weight loss stage initiating at ca. 324 °C was observed for EA, which was due to the pyrolysis of epoxypropyl group. Cellulose was thermally degraded in the range of 320–400 °C to generate H_2O, CO, CO_2, CH_4 and alkanols (Hiltunen, Siirilä, & Maunu, 2012).

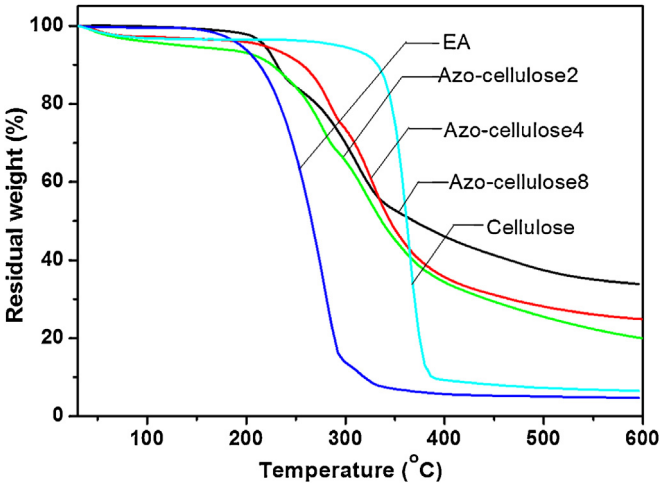

Fig. 3. TGA curves of EA, cellulose, and Azo-cellulose2, 4, 8 with DS_{azo} = 0.28, 0.60, 1.98, respectively.

The residual content of Azo-celluloses was 13–28% more than that of cellulose at 600 °C, and it increased with the DS_{azo} value of EA group, i.e. it was 20.1, 24.9 and 34.0% for Azo-cellulose2, 4, and 8, respectively. This is due to the flame-retardancy effect of azo compounds (Shen & Gu, 2009), leading to the production of more char residues.

The initial thermal decomposition temperature for Azo-cellulose2, 4 and 8 is 225, 249, and 213 °C, respectively. Thus the thermal stability of Azo-cellulose is 18–54 °C higher than that of EA. Two stages of weight loss are present for Azo-celluloses. The first stage appears at ca. 280 °C similar to that of EA. The second stage starting from 290 °C is due to the decomposition of cellulose main chains. Obviously the thermal stability of Azo-celluloses is lower than that of cellulose. This is because not only the low thermal decomposition temperature of azo groups, but the destruction of chain regularity of cellulose chains after the introduction of EA side groups. The connection between the thermal stability and crystallinity of cellulose has been reported by some researchers. For instance, the regenerated cellulose fibers and the electrospun cellulose nanofibers were less thermal stable than the raw cellulose (Quan, Kang, & Chin, 2010; Xiong, Li, Yu, Hu, & Liu, 2013). This was attributable to the lower crystallinity of regenerated cellulose fibers as compared to that of the raw cellulose.

3.5. Photochromic property of HA, EA and Azo-cellulose in DMAc solutions

Similar to the UV–vis spectra of HA and EA solutions, the typical Azo-cellulose8/DMAc solution shows a strong peak at ca. 350 nm and a weak peak at ca. 440 nm (Fig. 4a), corresponding to the respective $\pi-\pi^*$ and $n-\pi^*$ electron transition of *trans*-azobenzene structure, further confirming the presence of azo moieties on Azo-cellulose. It has been reported that, in the visible light, the *trans*- and *cis*- photoisomers of azobenzene coexist but the former is much more stable than the latter, thus the former is predominant in solution or in bulk material (Nicolas, Wilén, Roth, Pfaendner, & King, 2006).

The UV–vis spectra of a typical Azo-cellulose8/DMAc solution under irradiation of 365 nm UV light are shown in Fig. 5b. The intensity of the strong band at 350 nm progressively decreases with irradiation time, while that of the weak band at 440 nm increases concomitantly. The reason is that more and more *trans*- isomers transform to *cis*- ones with the progress of UV light irradiation. In this *trans-cis* photoisomerization process, the small increase at 440 nm is because both isomers display $n-\pi^*$ transition at the

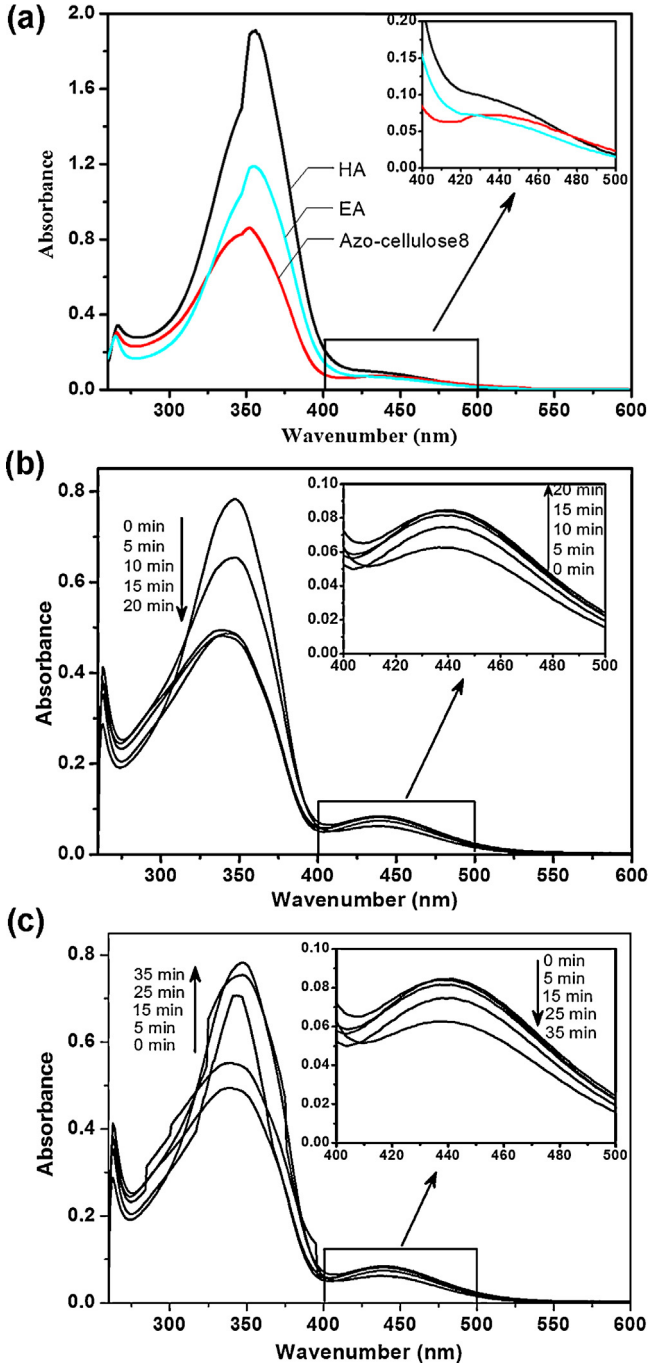

Fig. 4. (a) UV–vis spectra of HA, EA and Azo-cellulose8 (DS_{azo} = 1.98) in DMAc solution; UV–vis spectra of Azo-cellulose8/DMAc solutions after (b) 365 nm UV light and (c) visible light irradiation.

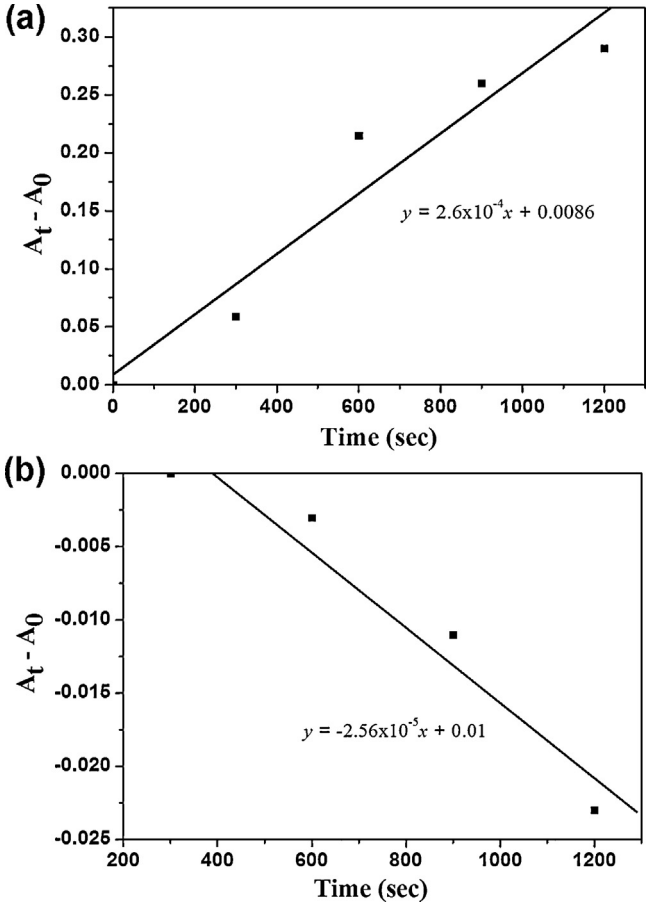

Fig. 5. Plots of absorbance change against irradiation time for the Azo-cellulose8 (DS_{azo} = 1.98)/DMAc solution under visible light irradiation. Absorbance change at (a) 340 nm and (b) 440 nm. A_0 and A_t were peak absorbance values at 0 min and irradiation time.

same wavelength of ca. 440 nm (Hurduc et al., 2007). The peak absorbance values vary very little since after irradiation for 10 min, suggesting that the photostationary state is reached. However, the photostationary state of our Azo-cellulose is different from that of some other azo-compounds. For instance, a liquid crystalline dendrimer with azobenzene terminal groups displayed no absorbance peak at 350 nm at photostationary state (Liu, Ni, Qiu, Hou, & Zhang, 2007). This is possibly related to the backbone structure, i.e. rigid main chain structure of cellulose or aromatic polymer may hamper the rotation of azobenzene moieties, whereas flexible molecule structure impart little resistance to the transformation of azobenzene moieties upon light irradiation (Hurduc et al., 2007; Jiang et al., 2010; Liu et al., 2007). Under visible light irradiation, the *cis*- band at 440 nm decreases, while the *trans*- band at 350 nm increases (Fig. 4c), indicating the occurrence of a reversible *cis-trans* isomerization. It takes ca. 25 min to reach complete reversibility, which is ca. 15 min longer than that for attaining the photostable *trans-cis* transition. Such a slower *cis-trans* reverse rate than *trans-cis* transition rate is a characteristic phenomenon for azo-bearing polymer (Hurduc et al., 2007). It should be pointed out the other Azo-cellulose/DMAc solutions show similar fully reversible *trans-cis-trans* transitions under successive irradiation of UV and visible light.

Due to the peak absorbance values in the course of *cis-trans* transition changed more steadily (Fig. 4c) than that of *trans-cis* transition (Fig. 4b), the kinetics of the *cis-trans* transition of Azo-cellulose in DMAc was further analyzed as an example by plotting the absorbance at 350 nm and 440 nm against irradiation time (Fig. 5). It is found that the content $(A_t - A_0)$ of *trans*-isomer increases, while that of *cis*-isomer decreases almost linearly with time under irradiation of visible light. Thus the photoinduced *cis-trans* transition of Azo-cellulose follows the first order kinetics, as found for many other azo-polymers (Hurduc et al., 2007; Liu et al., 2007). The photochromism rate constants, i.e. the slopes of the plots, are 2.6×10^{-4} and 2.56×10^{-5} s^{-1} for the π–π^* and n–π^* transition, respectively. The latter is one order of magnitude less than the former, suggesting the n–π^* transition is much less obvious than the π–π^* transition. The rate constant of our Azo-cellulose is of the same order as that of cyanophenylazophenol cellulose (Yang et al., 2001). However, the photoisomerization rate of

Azo-cellulose is about 10^3 times less than that of azo-polymer with a flexible aliphatic chain spacer (Liu et al., 2007), due to the steric hindrance of the semi-rigid main chain of cellulose.

Azobenzene group is a type of chromophore group, whose molecular structure have two isomers, i.e. *trans*- and *cis*-, they can reversely change under irradiation of light with suitable wavelength. Such a change leads to conformational switch between a rod-like shape of *trans*-isomer and a skewed shape of *cis*-isomer. Since the transition between the two isomers can be conveniently achieved by light irradiation, such azo-containing biopolymers with photochemically stimulated conformational change can be potentially used to fabricate motor, actuator, and artificial muscle (Yamada et al., 2008). Due to the good biocompatibility and mechanical property of backbone cellulose, the photochromic azo-cellulose ether might show potential applications in biomaterials.

4. Conclusions

We reported a fast and highly efficient introduction of photochromic azobenzene moieties onto cellulose molecular chains through etherification reaction in DMAc/LiCl solvent. The azo-cellulose ethers showed good solubility in most polar organic solvents. The thermal stability of Azo-celluloses was improved as compared to that of 2,3-epoxypropoxy-azobenzene (EA), but was ca. 30 °C less than that of cellulose. The Azo-cellulose/DMAc solutions displayed reversible *trans-cis-trans* photoisomerization under successive irradiation of 365 nm UV light and visible light. The cis-trans isomerization followed the first order transition. In the UV–vis spectrum, the peak intensity at 350 nm (for π–π^* transition of *trans*-isomer) and 440 nm (for n–π^* transition of *cis*-isomer) concomitantly depresses or increases under light irradiation.

Acknowledgements

This work is supported by the National Basic Research Program of China (2010CB732203), the Natural Science Foundation of Fujian Province (2010J06017), Research Fund for the Doctoral Program of Higher Education of China (No. 20123503110003), the National Natural Science Foundation of China (No. 50973019), and Program for New Century Excellent Talents in Fujian Province University (JA10059).

References

Arai, K., & Kawabata, Y. (1995). Preparation of triphenylcarbinol moiety-containing cellulose derivative and its properties. *Macromolecular Chemistry and Physics*, *196*, 2139–2147.

Arai, K., Shitara, Y., & Ohyama, T. (1996). Preparation of photochromic spiropyrans linked to methyl cellulose and photoregulation of their properties. *Journal of Materials Chemistry*, *6*, 11–14.

Asanuma, H., Liang, X., Nishioka, H., Matsunaga, D., Liu, M. Z., & Komiyama, M. (2007). Synthesis of azobenzene-tethered DNA for reversible photo-regulation of DNA functions: Hybridization and transcription. *Nature Protocols*, *2*(1), 203–212.

Barton, D., Hodgett, M., Skirving, P., Whelton, M., Winter, K., & Vardy, C. (1983). The thermal decomposition of azobenzene. *Canadian Journal of Chemistry*, *61*(8), 1712–1718.

Chang, C., & Zhang, L. (2011). Cellulose-based hydrogels: Present status and application prospects. *Carbohydrate Polymers*, *84*(1), 40–53.

Ciardelli, F., Bertoldo, M., Bronco, S., Pucci, A., Ruggeri, G., & Signori, F. (2013). The unique optical behaviour of bio-related materials with organic chromophores. *Polymer International*, *62*(1), 22–32.

Ercole, F., Davis, T. P., & Evans, R. A. (2010). Photo-responsive systems and biomaterials: Photochromic polymers, light-triggered self-assembly, surface modification, fluorescence modulation and beyond. *Polymer Chemistry*, *1*, 37–54.

Fox, S. C., Li, B., Xu, D., & Edgar, K. J. (2011). Regioselective esterification and etherification of cellulose: A review. *Biomacromolecules*, *12*(6), 1956–1972.

Glasser, W. G., Becker, U., & Todd, J. G. (2000). Novel cellulose derivatives. Part VI. Preparation and thermal analysis of two novel cellulose esters with fluorine-containing substituents. *Carbohydrate Polymers*, *42*(4), 393–400.

Hiltunen, M., Siirilä, J., & Maunu, S. L. (2012). Effect of catalyst systems and reaction conditions on the synthesis of cellulose-g-PDMAam copolymers by controlled radical polymerization. *Journal of Polymer Science Part A: Polymer Chemistry*, *50*(15), 3067–3076.

Hou, A., Zhang, C., & Wang, Y. (2012). Preparation and UV-protective properties of functional cellulose fabrics based on reactive azobenzene Schiff base derivative. *Carbohydrate Polymers*, *87*(1), 284–288.

Hua, X., Zheng, P. J., Zhao, X. Y., Li, L., Tam, K. C., & Gan, L. H. (2004). Preparation, characterization and novel photoregulated rheological properties of azobenzene functionalized cellulose derivatives and their alpha-CD complexes. *Polymer*, *45*, 6219–6225.

Hurduc, N., Adès, D., Belleney, J., Siove, A., & Sauvet, G. (2007). Photoresponsive new polysiloxanes with 4-substituted azobenzene side-groups. Synthesis, characterization and kinetics of the reversible trans-cis-trans isomerization. *Macromolecular Chemistry and Physics*, *208*(24), 2600–2610.

Jiang, X., Wang, H., Chen, X., Li, X., Lei, L., Mu, J., et al. (2010). A novel photoactive hyperbranched poly(aryl ether ketone) with azobenzene end groups for optical storage applications. *Reactive and Functional Polymers*, *70*(9), 699–705.

Kondo, T., & Gray, D. G. (1991). The preparation of O-methyl- and O-ethyl-celluloses having controlled distribution of substituents. *Carbohydrate Research*, *220*, 173–183.

Li, M. H., Keller, P., Li, B., Wang, X. G., & Brunet, M. (2003). Light driven side-on nematic elastomer actuator. *Advanced Materials*, *15*, 569–572.

Liu, J., Ni, P., Qiu, D., Hou, W., & Zhang, Q. (2007). Photochromism of liquid crystalline dendrimer with azobenzene terminal groups in solution. *Reactive and Functional Polymers*, *67*(5), 416–421.

Nicolas, R. C., Wilén, C.-E., Roth, M., Pfaendner, R., & King, R. E. (2006). Azoalkanes: A novel class of flame retardants. *Macromolecular Rapid Communications*, *27*(12), 976–981.

Nishi, H., Namari, T., & Kobatake, S. (2011). Photochromic polymers bearing various diarylethene chromophores as the pendant: Synthesis, optical properties, and multicolor photochromism. *Journal of Materials Chemistry*, *21*(43), 17249–17258.

Oertel, U., Mart, H., Komber, H., & Bohme, F. (2009). Media effects on the optical properties of proton donor group containing azobenzene derivatives. *Optical Materials*, *32*(1), 54–61.

Pieroni, O., Fissi, A., Angelini, N., & Lenci, F. (2000). Photoresponsive polypeptides. *Accounts of Chemical Research*, *34*(1), 9–17.

Quan, S.-L., Kang, S.-G., & Chin, I.-J. (2010). Characterization of cellulose fibers electrospun using ionic liquid. *Cellulose*, *17*(2), 223–230.

Sahu, M., Saha, M. B., & Bera, S. C. (1995). Azo-hydrazo tautomerization and cis-trans isomerization of 2-carboxy-2′-hydroxy-4′-methyl azobenzene. *Journal of Photochemistry and Photobiology A: Chemistry*, *89*(1), 19–24.

Shen, D. K., & Gu, S. (2009). The mechanism for thermal decomposition of cellulose and its main products. *Bioresource Technology*, *100*(24), 6496–6504.

Song, Y. B., Sun, Y. X., Zhang, X. Z., Zhou, J. P., & Zhang, L. N. (2008). Homogeneous quaternization of cellulose in NaOH/urea aqueous solutions as gene carriers. *Biomacromolecules*, *9*(8), 2259–2264.

Xiong, R., Li, F., Yu, J., Hu, P., & Liu, Z. (2013). Preparation and properties of fibers produced from a cellulose/complex PA solvent system precipitating in diverse coagulants. *Fibers and Polymers*, *14*(6), 926–934.

Xue, X., Zhu, J., Zhang, W., Zhang, Z., & Zhu, X. (2009). Preparation and characterization of novel main-chain azobenzene polymers via step-growth polymerization based on click chemistry. *Polymer*, *50*(19), 4512–4519.

Yamada, M., Kondo, M., Mamiya, J. I., Yu, Y. L., Kinoshita, M., Barrett, C. J., et al. (2008). Photomobile polymer materials: Towards light-driven plastic motors. *Angewandte Chemie-International Edition*, *47*(27), 4986–4988.

Yang, S. Z., Jacob, M. M., Li, L., Cholli, A. L., Kumar, J., & Tripathy, S. K. (2001). Synthesis and characterization of novel azobezene-modified polymers: Azocellulose. *Macromolecules*, *34*(26), 9193–9196.

Yashima, E., Noguchi, J., & Okamoto, Y. (1995). Photocontrolled chiral recognition by [4-(phenylazo)phenyl]carbamoylated cellulose and amylose membranes. *Macromolecules*, *28*, 8368–8374.

Yu, B., Jiang, X., Wang, R., & Yin, J. (2010). Multistimuli responsive polymer nanoparticles on the basis of the amphiphilic azobenzene-contained hyperbranched poly(ether amine) (hPEA-AZO). *Macromolecules*, *43*(24), 10457–10465.

Zhang, D., Xie, J., Yu, P., Huang, X. K., Yang, M. H., & Liu, H. Q. (2012). Antifungal activity and humidity sensitivity of quaternized cellulose synthesized in NaOH/urea aqueous solution. *Cellulose*, *19*(1), 189–198.